DEVELOPMENT OF NEW BRIDGE RESTRAINER USING LAMINATED FIBER REINFORCED RUBBER

Nobutaka Ishikawa[1], **Yasushi Nishimoto**[1] **and Toru Ukishima**[2]
[1]*National Defense Academy, Yokosuka 238-0022, Japan*
E-mail: cgishikawa@m4.dion.ne.jp
[2]*Shibata Industrial Co. Ltd., Akashi 674-0082, Japan*

Abstract

This paper presents an experimental approach for the development of new bridge restrainer system using laminated fiber reinforced rubber (LFRR). After Kobe earthquake on January 1995, the design concept for the bridge restrainer has been revised so that the bridge should install the shock absorber which may be prevented from falling down due to earthquake shock. However, the shock absorbing system for the bridge restrainer has been required to satisfy the two performance requirements of high energy absorption and reduction of impact load. To this end, the laminated fiber reinforced rubber was developed to apply to the new bridge restrainer system as a shock absorber. In this study, the three kinds of tests of static compression, rapid speed loading and weight dropping impact for the LFRR specimen were first performed in order to investigate the efficiency of LFRR as a shock absorber. Then, the rubber-rolled pin was also developed as a new bridge restrainer system from the viewpoints of impact load reduction and high energy absorption.

Keywords: bridge restrainer, laminated fiber reinforced rubber, impact test, shock absorber

1. Introduction

As one of many fallout accidents of bridge girders occurred by the Kobe earthquake on January 1995 in Japan (Kawashima et al., 1997), the bridge restrainer system was damaged by impulsive loading in many places. Thus, the new bridge restrainer system has become needed to develop the shock absorbing device in order to prevent it from the failure if the equivalent earthquake occurs (Japan Road Association, 1996). In case of severe earthquake, a shock absorber is required to reduce the impact load which acts on the falling down prevention devices and also to absorb the high kinetic energy of girders. However, it is difficult to satisfy these two performance requirements at the same time. Although the high stiffness of a material is required in order to absorb the kinetic energy, it can not reduce the impact load. Therefore, a new shock absorber using the laminated fiber reinforced rubber (LFRR) is developed as shown in Figure 1 (Nishimoto et al., 2000, 2001).

In this study, the efficiency of LFRR is first investigated by performing three kinds of tests (static compression, rapid speed loading and weight dropping impact tests) from the viewpoints of two performance requirements of impact load reduction and high energy absorption. Second, the rubber-rolled pin using LFRR is developed as a new bridge restrainer by carrying out the impact

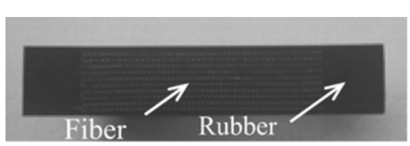

Fig. 1. LFRR.

M. Pandey et al. (eds), Advances in Engineering Structures, Mechanics & Construction, 809–821.
© 2006 *Springer. Printed in the Netherlands.*

Table 1. Material properties of laminated fiber reinforced rubber.

	Fiber			Rubber	
	High tension (HMF)	Middle tension (MMF)	Low tension (LMF)	Hardness degrees of 50 (R50)	Hardness degrees of 65 (R65)
Material	6-nylon	6,6-nylon	Vinylon	Natural rubber	
Tensile strength	5292(N/3cm)	2646(N/3cm)	1764(N/3cm)	10.2(MPa)	20(MPa)
Elongation percentage at break	40(%)	25(%)	20(%)	600(%)	600(%)

Table 2. Test cases.

Specimen	Static compression test	Rapid speed loading test	Weight dropping test
R50	○	○	○
R65	○	○	○
LMF1	○		
LMF5	○	○	○
LMF25	○	○	○
LMF50	○		
MMF1	○		
MMF5	○	○	○
MMF25	○		
MMF50	○		
HMF1	○		
HMF5	○	○	○
HMF25	○		

test (Ishikawa et al., 1997). Finally, effects of LFRR and rubber-rolled pin are discussed from the viewpoints of mitigation of impact load and the energy absorption.

2. Effect of Laminated Fiber Reinforced Rubber (LFRR) as Shock Absorber

2.1. *Specimen and Test Cases of LFRR*

The shape of specimen of LFRR is a rectangular cross section with length of 150 mm, wide of 150 mm and depth of 50 mm. The LFRR is consisted of rubber with hardness degrees of 50, 65 and three kinds of fiber which are 6-Nylon (HMF), 6,6-Nylon (MMF) and Vinylon (LMF) with different tensile strength as shown in Table 1. Test cases are shown in Table 2 in which R50 and R65 stand for the rubber with hardness degree of 50 and 65, respectively and LMF5 means the laminated fiber reinforced rubber with five pieces of low tensile strength fiber.

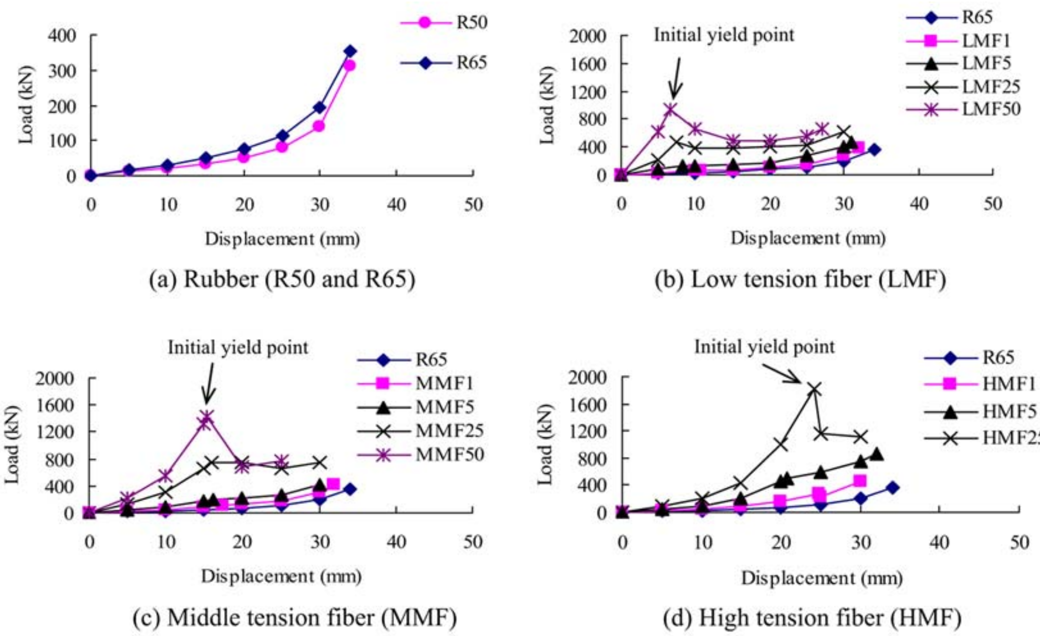

(a) Rubber (R50 and R65) (b) Low tension fiber (LMF)

(c) Middle tension fiber (MMF) (d) High tension fiber (HMF)

Fig. 2. Load ∼ displacement curve by static compression test.

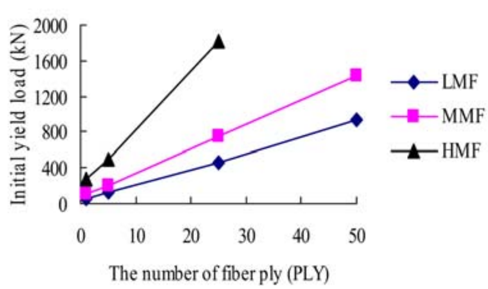

Fig. 3. Initial yield load ∼ fiber ply relation.

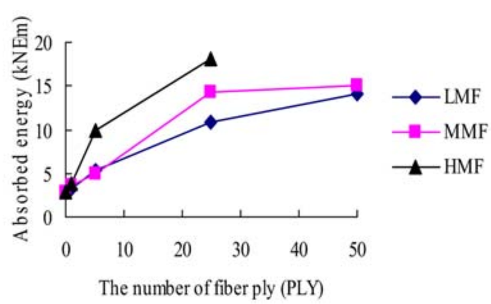

Fig. 4. Absorbed energy ∼ fiber ply relation.

2.2. *Static Compression Test*

The static compression test was performed by using the 5,000 kN compression test machine.

Figure 2 shows the load-displacement relations by static compression test. The arrow in Figure 2 indicates the initial yield point at which the laminated fiber starts to break. It is found that the load-displacement curves of the LFRR show the elastic-plastic behavior and these are obviously different from those of the usual rubber. Figures 3 and 4 illustrate the initial yield load – the number of fiber ply relation and absorbed energy – the number of fiber ply relation, respectively. It can be seen that the initial yield load and the absorbed energy of LFRR increase with the increase of the number of fiber ply. Therefore, if we want to obtain the required initial yield load, we can select the number of fiber with an appropriate tensile strength. It is also noticed from Figure 4 that the absorbed energy (18 kN·m) of HMF (25 PLY) is about 6 times larger than that (3 kN·m) of usual rubber (0 PLY).

Fig. 5. Rapid speed loading machine.

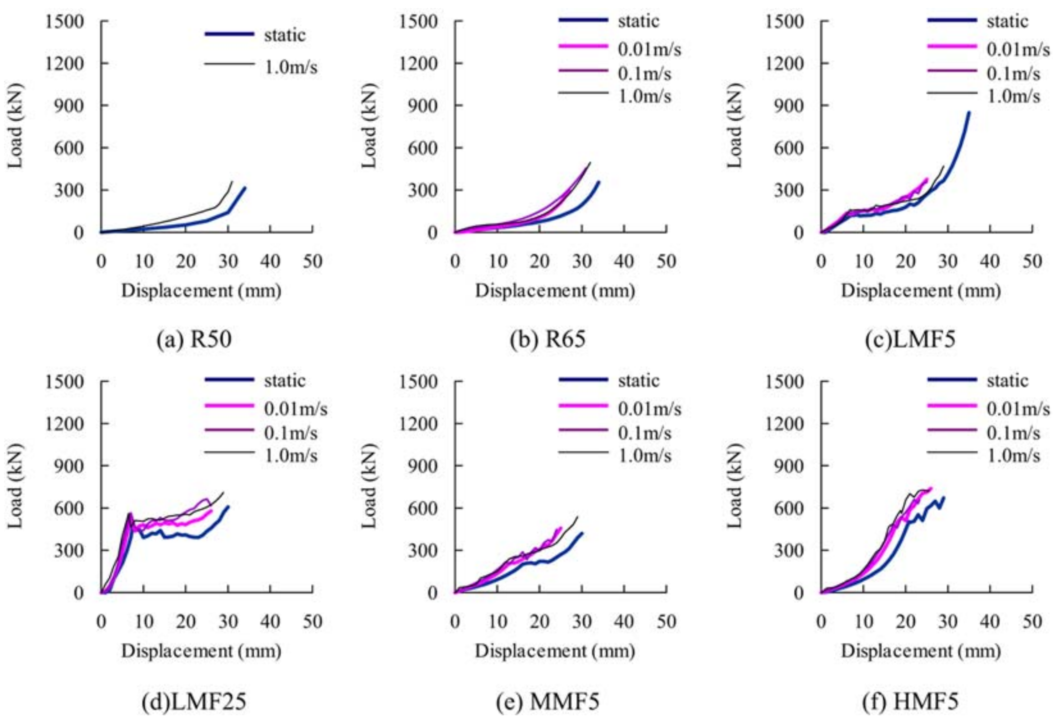

Fig. 6. Load ∼ displacement curve by rapid speed loading test.

2.3. *Rapid Speed Loading Test*

The rapid speed loading test was executed by using the rapid loading machine as shown in Figure 5. The aim of this dynamic test is to examine the rate-effect of LFRR and the loading speed was set at 0.01 m/sec, 0.1 m/sec and 1.0 m/sec. The load was measured by the 1,000 kN load cell and the displacement was measured by the laser type displacement sensor.

Figure 6 shows the dynamic load-displacement relations including static compression test results. It is found that the loading speed has remarkable effect on the load-displacement relation in case of

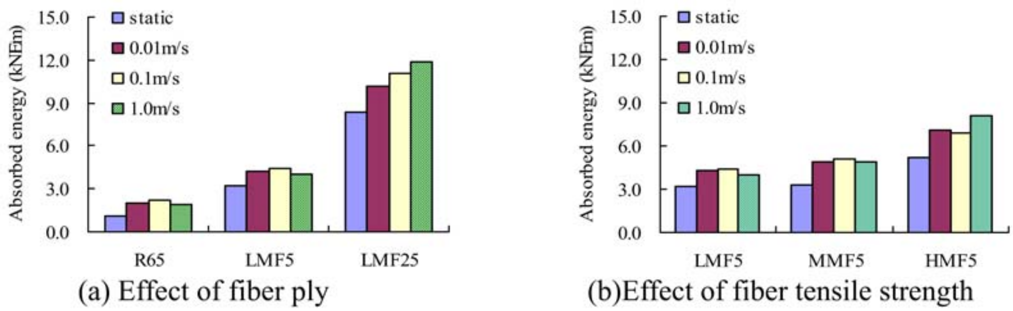

Fig. 7. Absorbed energy ~ loading speed relations.

Fig. 8. Weight dropping machine.

usual rubber when the displacement exceeds 10 mm. For example, the dynamic load is about 2.5 times larger than the static load at the displacement of 25 mm.

It is also noticed that from Figures 6c–6f that the initial yield load increases about 20%, but in plastic region after initial yield load, the dynamic load increases about 30–50% larger than the static one in case of LFRR. This may be caused that fiber breaks gradually and the LFRR becomes like the usual rubber. These facts mean that the usual rubber tends to be more sensitive in rate effect than LFRR.

Figure 7 represents the absorbed energy of LFRR and it is obvious that the absorbed energy of LMF25 in case of rapid speed loading (1.0 m/sec) becomes larger than those of R65, LMF5. It is also noticed that the absorbed energy increases as the fiber ply and fiber tensile strength increase.

2.4. *Weight Dropping Impact Test*

The weight dropping impact test was carried out by using the weight dropping machine as shown in Figure 8. The falling weight was set at $W = 4.0$ kN and the falling height was set at $H = 0.25$, 1.25 and 2.5 m ($V = 2.21$, 4.94 and 7.00 m/sec), that is, impact energy was set at $E = 1.0$, 5.0

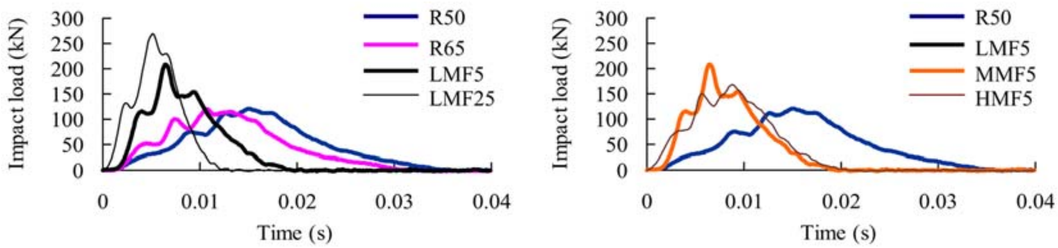

(a) Rubber (R50 and R60) and LMF (b) R50 , LMF5, MM5 and HMF5

Fig. 9. Impact load ∼ time relation (input energy $E_i = 1.0$ kN·m).

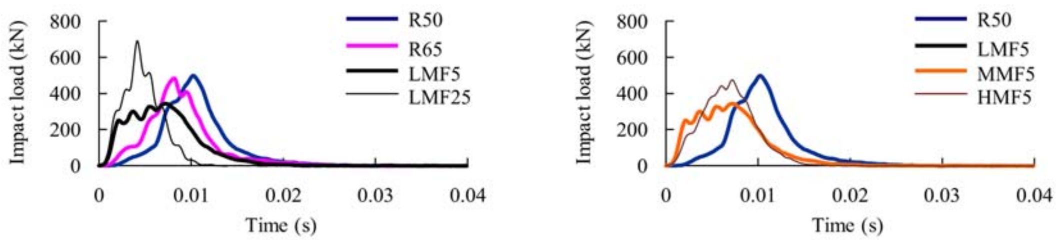

(a) Rubber (R50 and R60) and LMF (b) R50 , LMF5, MM5 and HMF5

Fig. 10. Impact load ∼ time relation (input energy $E_i = 5.0$ kN·m).

and 10.0 kN·m. These mean that $E = 1.0$ kN·m is the energy that laminated fiber may never break, $E = 10.0$ kN·m is the energy that laminated fiber may break perfectly and $E = 5.0$ kN·m is the intermediate value between 1.0 and 10.0 kN·m. These energies are determined by the results of static compression test. The impact transmitted load is measured by using the 2,000 kN load cell attached at the steel plate under the specimen.

Figures 9, 10 and 11 illustrate the load-time relations obtained by weight dropping impact test. It can be seen from Figure 9 that the maximum impact transmitted load of LFRR is larger than the one of usual rubber and the impact duration time of LFRR is shorter than that of usual rubber in case of low input energy $E = 1.0$ kN·m. This may be the reason why the stiffness of LFRR in elastic region is larger than that of usual rubber. However, it should be noticed from Figures 10 and 11 that the maximum impact load of LFRR at large input energy becomes smaller than that of usual rubber.

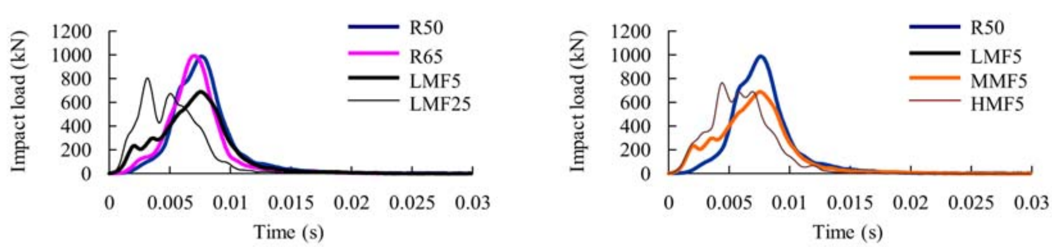

(a) Rubber (R50 and R60) and LMF (b) R50 , LMF5, MM5 and HMF5

Fig. 11. Impact load ∼ time relation (input energy $E_i = 10.0$ kN·m).

Table 3. Maximum impact load.

	1.0kN • m	5.0kN • m	10.0kN • m
R50	120.6	497.7	987.7
R65	114.8	482.3	991.5
LMF5	203.8	326.3	687.1
LMF25	268.9	690.0	803.9
MMF5	167.5	414.4	670.9
HMF5	168.4	474.7	765.6

Table 4. Energy absorption ratio.

Specimen	Energy absorption ratio (%)	
	Ei=1.0kN · m	Ei=10.0kN · m
R65	72.1	85.0
LMF5	86.6	88.7
LMF25	88.9	90.4
MMF5	89.3	87.8
HMF5	86.5	85.5

The reason why the maximum load of LFRR is reduced may be due to that the LFRR can absorb the large kinetic energy by breaking the laminated fiber and decreasing the stiffness.

Table 3 shows the maximum impact load and the hatching figures mean that the laminated fiber breaks. For instance, the maximum loads of LMF5 in cases of $E = 5.0$ kN and 10.0 kN·m are 1/1.5 smaller those of usual rubber R65. Therefore, the LFRR is effective as a shock absorber rather than usual rubber from the viewpoint of the mitigation effect of impact load at high input energy.

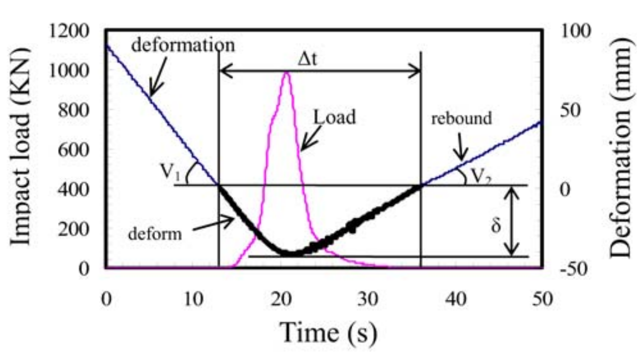

Fig. 12. Impact load, deformation-time relation. (R50) $E = 10.0$ kN·m.

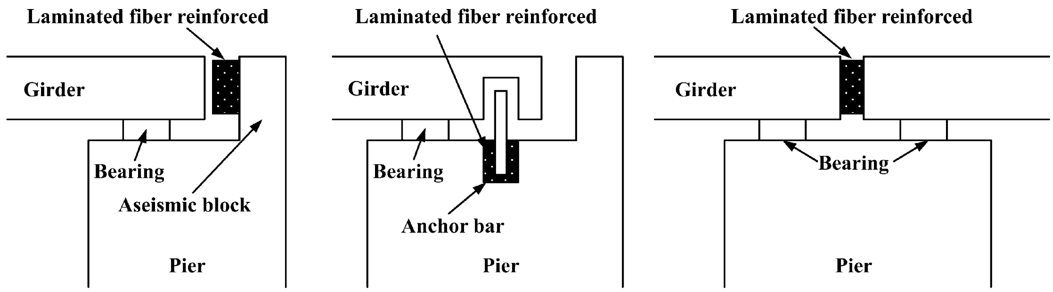

Fig. 13. Direct application of LFRR to bridge restrainer system.

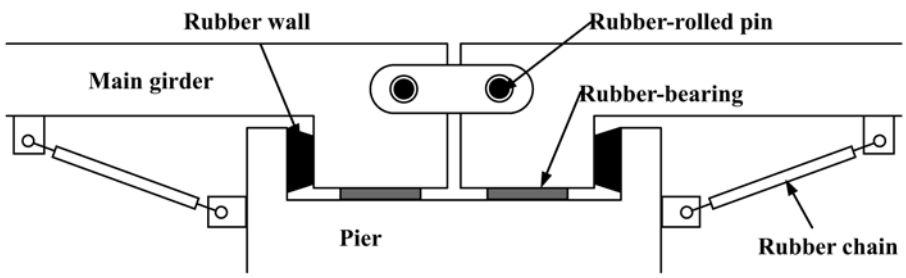

Fig. 14. Indirect application of LFRR to bridge restrainer system.

Table 4 expresses the energy absorption ratio (ΔE) which is defined as follows:

$$\Delta E = \frac{E - E'}{E} \times 100\%, \tag{1}$$

in which E and E' are the kinetic energy before and after collision, respectively. The velocity of weight is obtained by differentiating the traveling distance with respect to time as shown in Figure 12. It can be seen from Table 4 that the energy absorption ratio of LFRR is larger than that of natural rubber in every cases. Therefore, the LFRR can absorb the kinetic energy of weight, that is, the velocity of the weight (girder) after collision in case of LFRR becomes smaller than that of usual rubber. This means that the damage of girder using the LFRR may be smaller than that using usual rubber.

3. Application to New Bridge Restrainer System

The LFRR is directly applied to the shock absorber of aseismic block, anchor bar and pounding between girders as shock absorbers of new bridge restrainer system as shown in Figure 13.

However, it is difficult to prevent the fallout accident of girder by only one shock absorber in case of large scale earthquake. Therefore, it would be desirable that a bridge structure may be installed by combining various kinds of shock absorbing system such as rubber wall, rubber-bearing, rubber-pin and rubber chain as shown in Figure 14. For instance, the rubber chain device and rubber wall using LFRR might be useful as devices which can absorb large amount of energy for the huge earthquake.

Furthermore, the rubber-rolled pin would improve the existing bridge restrainer plate system as device which can mitigate the transmitting load to girders.

Herein, the effect of rubber-rolled pin is examined by performing the impact test from the viewpoints of mitigation of impact load and the energy absorption.

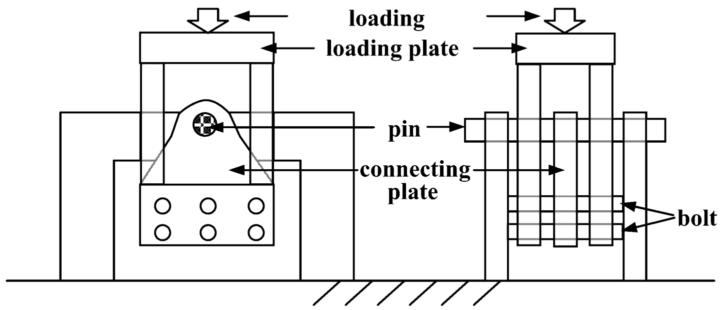

Fig. 15. Impact test of rubber-rolled pin.

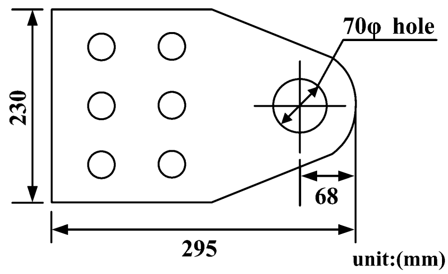

Fig. 16. Connecting plate.

3.1. *Impact Loading Test of Rubber-Rolled Pin*

The impact loading test using dropping weight machine was carried out by pushing down the loading plate which was linked with the connecting plate by bolts as shown in Figure 15. The steel pin and rubber-rolled pin pass through the connecting plate and cut them off by pushing down the loading plate. The connecting plate specimen (SS400, thickness 9 mm) is a half size of actual shape as shown in Figure 16 and its cross section is equal to the connecting plate which is used in the bridge of about 20 m span length. The pin specimens (SC35) were used as two types as shown in Table 5. Type A is the ordinary steel pin and type B is the rubber-rolled pin using LFRR in which they have the same total diameter of 60 mm. The load was measured by the load cell and displacement was measured by the laser type sensor, respectively. In impact test, the responding strains of connecting plate were measured by the 3-axial gauges which were arranged as shown in Figure 17.

The falling weight was set at $W = 1$ kN and falling height was set at $H = 10$–150 cm (impact velocity $V = 140$–540 cm/sec).

3.2. *Load Mitigation Effect of Rubber-Rolled Pin*

Figure 18 shows the circumferential strain-time relations at interval of 30° in the elastic range ($W = 1$ kN, $H = 10$ cm). It is found that the maximum strain (350 μ) at No. 7 ($\theta = 90°$) of type-B becomes about 1/4 smaller than the one (1350 μ)of type-A. It is also confirmed that the difference of the maximum strain at each position of type-B is smaller rather than the one of type-A (for example, the difference of No. 1 and No. 7 in type-B is about 40%, but it is about 75% in type-A). It is guessed that this phenomenon may be caused by the larger contact area between rubber-rolled pin and plate in type-B. Thus, type-B can disperse the transmitting load to connecting plate. Therefore, the rubber-

Table 5. Type of pin (unit:mm).

pin-type	type-A (steel-pin)	type-B (rubber-rolled pin)
cross section	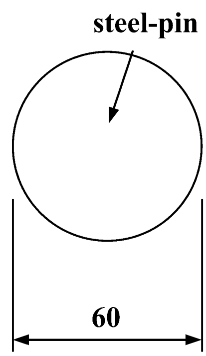	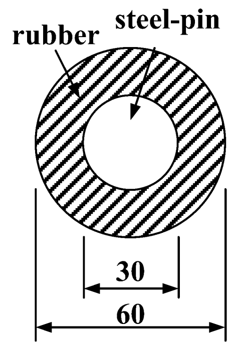

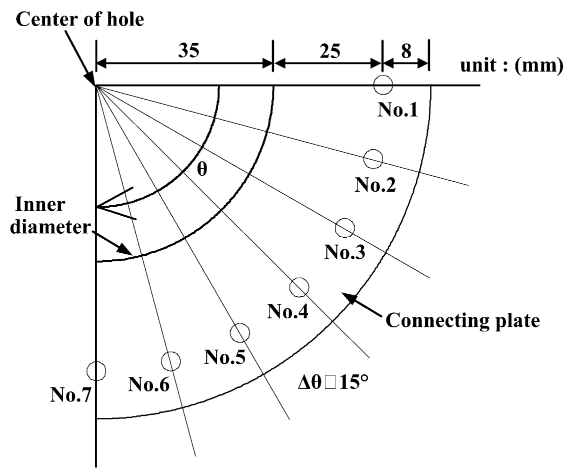

Fig. 17. Position of strain gauges.

rolled pin can expect not only the effect of mitigating impact load, but also the effect of dispersing impact load. This tendency was also confirmed in the radial components of strains.

Figure 19 shows the strain (at gauge No. 7) – time relations at $W = 1$ kN and $H = 10$ cm. It is apparent that the maximum strain of type-B is about 1/3–1/4 smaller than the one of type-A, and the responding period of radial strains of type-B is about twice as long as type-A. Therefore, type-B can prevent the stress concentration of connecting plate in elastic range.

3.3. *Energy Absorption of Rubber-Rolled Pin*

In the previous test, the load mitigation effect of rubber-rolled pin was examined within the elastic loading range. Next, the dropping height is increased from 10 cm to 150 cm and the elastic limit height was judged as the state of permanent strain remained obviously.

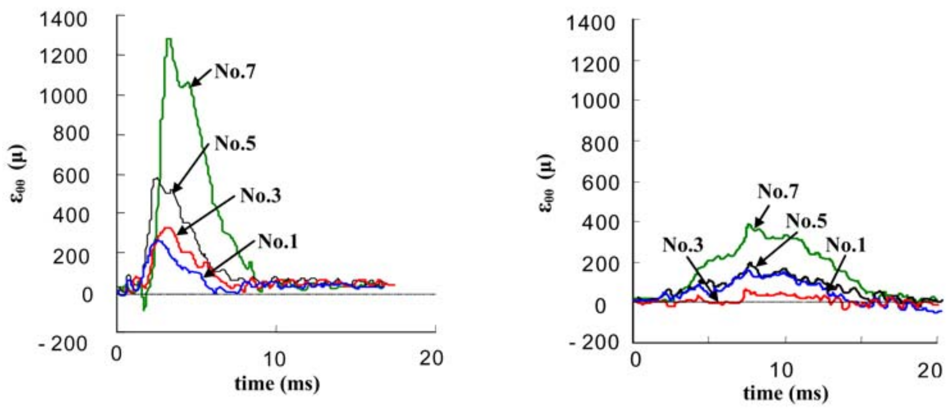

(a) Type-A (steel pin) **(b) Type-B (rubber-rolled pin)**

Fig. 18. Circumferential strain-time relations.

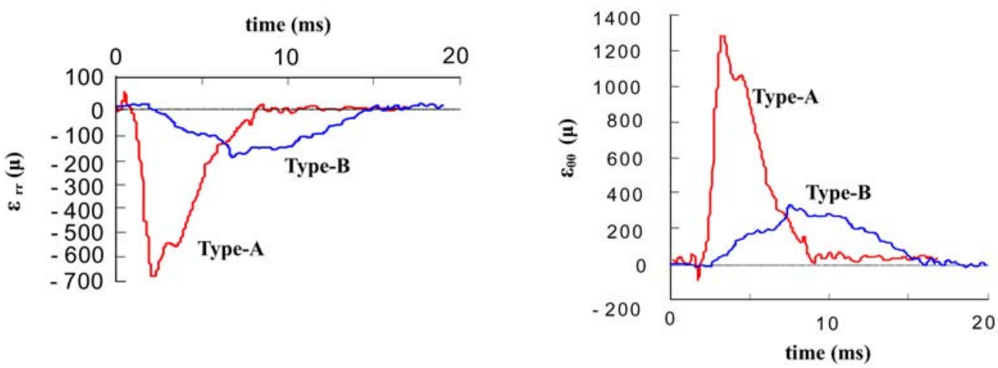

(a) radial strains **(b) circumferential strains**

Fig. 19. Strain (No. 7) – time relations at $W = 1$ kN, $H = 10$ cm.

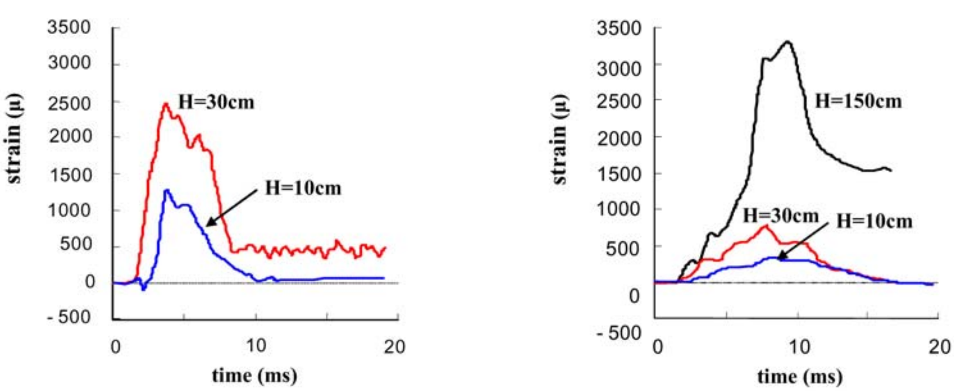

(a) Type-A **(b) Type-B**

Fig. 20. Strain (No. 7) – time relation at various falling height.

Figure 20 illustrates the strain (No. 7) – time relations by increasing the dropping height until the elastic limit state. It is found that the effect of mitigating the load at elastic limit level is similar to the previous elastic range, that is, the strain of 2500 μ at $H = 30$ cm of type-A is reduced to 800 μ (70% reduction) at $H = 30$ cm of type-B. It is also noticed that the elastic limit state of type-B ($H = 150$ cm) exhibits five times larger than the one of type-A ($H = 30$ cm). Therefore, the energy absorption of type-B has five times larger than the one of type-A, and therefore, type-B will be able to work under the elastic-plastic range of connecting plate for the considerable severe loading condition.

4. Conclusions

The following conclusions are drawn from this study.

4.1. *Development of LFRR*

(1) The maximum impact load of the LFRR in case of high kinetic energy is smaller than that of usual rubber, although its stiffness is large. Because, the LFRR can reduce the impact load by breaking the fiber in the rubber in case of high kinetic energy.
(2) The energy absorption ratio of LFRR is larger than the one of usual rubber. Therefore, the velocity after collision in case of LFRR becomes smaller than that of usual rubber, and such, the damage of bridge may be reduced for the earthquake shock.
(3) The LFRR is much better materials than usual rubber from the viewpoints of high absorbed energy and reducible effect of impact load at high input energy. Therefore, the LFRR is directly applied to the shock absorber of bridge restrainer system.

4.2. *Development of Rubber-Rolled Pin*

(1) The rubber-rolled pin exhibits obviously the mitigating effect of transmitting load to girders. This rate becomes smaller about 1/3–1/4 of the ordinary steel pin from the responding strains.
(2) The rubber-rolled pin has the transmitting and dispersing effects which would prevent the stress concentration of connecting plate in elastic and elastic-limit range.
(3) The energy absorption of rubber-rolled pin is about five times larger than the one of the ordinary steel pin. Thus, the rubber-rolled pin is advantageous as a bridge restrainer system for the severe loading condition.

References

Ishikawa, N., Sonoda, Y. and Hikosaka, H., 1997, Development of New Bridge Restrainer with Rubber-Rolled Pin for the Great Earthquake, *Earthquake Resistant Engineering Structures, Computational Mechanics Publications*, pp. 203–212.

Japan Road Association, 1996, Design Specification of Highway Bridge, Part V: Seismic Design [in Japanese].

Kawashima, K. and Unjoh, S., 1997, Impact of Hanshin/Awaji Earthquake on Seismic Design and Seismic Strengthening of Highway Bridge, *Journal of Structural Mechanics and Earthquake Engineering*, No. 556/I-38, pp. 1–30.

Nishimoto, Y., Kajita, Y., Ishikawa, N. and Nishikawa, S., 2000, An Experimental Study on Dynamic Properties of Laminated Fiber Reinforced Rubber as Shock Absorber of Bridge Restrainer System, *Journal of Structural Engineering*, Vol. 46A, pp. 1865–1874 [in Japanese].

Nishimoto, Y., Kajita, Y., Ishikawa, N. and Nishikawa, S., 2001, A Study on the Weight Dropping Impact Test and Prediction of the Impact Transmitted Load of Laminated Fiber Reinforced Rubber as a Shock Absorber for Bridge Restrainer System, *Journal of Structural Engineering*, Vol. 47A, pp. 1655–1664 [in Japanese].